***Paper ID: ICMIME2024_Paper No.:58***

# "Mathematical Modeling and Numerical Analysis of Natural Convection in a Nanofluid-Filled Prismatic Enclosure with Validation and Flow-Field Investigation"

Tamzid Abdullah[1], Sheikh Ittehad Uddin[1]
[1]Department of Mechanical Engineering, Chittagong University of Engineering & Technology,
Chittagong-4349, Bangladesh
*E-mail: tamzidabdullah2000@gmail.com[1], sheikhittehaduddinrafsan@gmail.com[1]*

## Abstract

*This research investigates natural convection heat transfer in a prismatic enclosure filled with water-based $Al_2O_3$ nanofluid, incorporating an oblong heat source at the bottom. The study is motivated by applications in attic-shaped buildings to enhance thermal comfort while minimizing energy costs associated with heating and cooling systems. The enclosure's heat source is modeled under isothermal, non-isothermal, and sinusoidal heating conditions, with adiabatic surfaces adjacent to the source and constant low temperatures on the inclined top walls. Governing equations, including non-dimensional Navier-Stokes and energy equations, are solved using the Finite Volume Method (FVM) via ANSYS Fluent v23. The results reveal that increasing the Rayleigh number ($10^3$–$10^7$) significantly enhances the average Nusselt number and improves convective heat transfer. Additionally, the inclusion of 4% volume fraction $Al_2O_3$ nanoparticles in water boosts heat transfer. Sinusoidal heating demonstrates superior nanofluid mixing, optimizing heat transfer performance*

Keywords: FVM, Rayleigh number, Nusselt number.

## "1. Introduction"

Convection is the mode of energy transfer between a solid surface and the adjacent liquid or gas that is in motion and it involves the combined effects of diffusion and advection due to fluid motion. Convection describes the movement of particles causes fluid density variation. Natural convection occurs when fluid move due to buoyancy force. Natural convection's low fluid velocity leads to a low heat transfer coefficient. The combination of conduction and convection heat transfer is widely utilized in natural and engineering scenarios, including solar thermal systems, electronic devices, chemical reactors, and building infrastructure, garnering considerable research attention. In recent years, many researchers interested in cavities due to their numerous applications. Recent literature reports several studies investigating internal natural convection in closed cavities filled with nanofluid and varying cavity shapes [1].

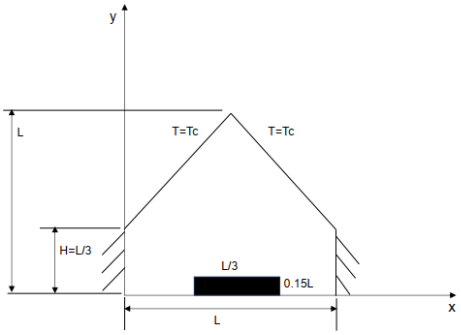
Tanmay et al. [2] studied natural convection in trapezoidal enclosures with different heating conditions on the bottom walls and isothermal side walls inclined at angle φ. Their numerical simulations showed that for non-uniform heating, the average heat transfer rate stays nearly constant across various tilt angles. Oliveski et al. [3] found that in rectangular cavities, entropy generation increases linearly with aspect ratio and irreversibility coefficient, and exponentially with Rayleigh number, with viscous effects further amplifying entropy generation at higher Rayleigh numbers. Jou and Tzeng [4] conducted a numerical study on nanofluids in rectangular enclosures, noting an increase in the average heat transfer coefficient with higher volume fractions, though the Nusselt number showed conflicting behavior. Raisi et al. [5] investigated conjugate heat transfer in a square enclosure with Cu-water nanofluid and a central heat-generating body, finding that higher solid volume fraction, Rayleigh number, and length ratio enhanced thermal performance and heat transfer rates. Solomon et al. [6] studied the effect of nanofluid concentration on natural convection in a square cavity with selective wall heating and cooling, finding that adding titanium dioxide nanoparticles enhanced heat transfer, with an optimal concentration for maximum improvement. Shuja et al. [7] examined heat transfer characteristics and irreversibility generation in a square vented cavity with a heat-generating body, considering the influence of exit port locations and aspect ratio. Farhadi et al. [8] employed the Lattice Boltzmann Method to examine natural convection in a square cavity with nanofluids, finding that increasing the solid volume fraction of water-based nanofluids ($Al_2O_3$ or Cu nanoparticles) enhanced the average Nusselt number, with Cu nanoparticles having a greater impact than $Al_2O_3$. Alam et al.'s study [9] examined how a prismatic enclosure's bottom wall condition affected heat transport

and heatline visualization. Aich and Omri [10] initially studied heat transfer in a prismatic cavity, revealing significant influence of the enclosure shape on thermal and flow fields. Quintino et al. [11] numerically investigated natural convection of nanofluids in a square cooled cavity with a heated horizontal cylinder, observing a periodic flow near one of the cooled walls when the cylinder is placed nearby. Yaseen [12] investigated the impact of strip heater placement and the number of heaters on flow and thermal fields within a prismatic cavity, revealing significant effects.

This study aims to develop and numerically solve a mathematical model of natural convection in a prismatic enclosure using the Finite Volume Method. The model is validated against existing literature and used to analyze flow and thermal behavior through streamline and isotherm plots, focusing on the impact of nanofluids and heat source configurations on heat transfer enhancement. Existing studies on nanofluids for heat transfer enhancement rarely address prismatic enclosures with bottom heat sources. The effects of heat source configurations and nanofluid properties on convection patterns and thermal performance remain underexplored, highlighting the need for a comprehensive investigation in this area.

## "2. Model Description"

A schematic geometry of the present problem has been shown in Figure 1. The entire cavity has been filled with air/nanofluid. Fixed room temperature has been maintained by inclined walls ($T_c$), which is lower than the heat source temperature. The lower horizontal part of the enclosure has been assumed to be an adiabatic wall. The two vertical side walls are insulated. The enclosure made of Aluminium is presumed in accessible.




$T(x)=T_h$ or,

$T(x)=T_c+(T_h-T_c)\sin(\pi x/L)$ or,

$T(x)=T_c+(T_h-T_c)(1-x/L)$

**Fig. 1:** Schematic diagram of the prismatic enclosure along with boundary conditions.

In this present study, the flow of air, nanofluid and water is assumed to be two dimensional, laminar and steady state within the enclosure. Heat transfer and fluid flow in an enclosure is governed by Navier–Stokes and Energy equation according to boundary condition. The entropy generation and heat transfer in the enclosure will be shown graphically by dimensionless parameters with varying Rayleigh number from $10^3$ to $10^7$ and solid-volume fraction of nanoparticles of $\phi$= 4%. The properties of fluid are characterized by three governing equations. The working fluid in this investigation are air and nanofluids. From the above approximations, governing equation for the present problem in non-dimensional form can be written as :

$$\frac{\partial U}{\partial X}+\frac{\partial V}{\partial Y}=0 \tag{1}$$

$$U\frac{\partial U}{\partial X}+V\frac{\partial U}{\partial Y}=-\frac{\partial P}{\partial X}+\frac{\mu_{nf}}{\rho_{nf}\alpha_f}\left(\frac{\partial^2 U}{\partial X^2}+\frac{\partial^2 U}{\partial Y^2}\right) \tag{2}$$

$$U\frac{\partial V}{\partial X}+V\frac{\partial V}{\partial Y}=-\frac{\partial P}{\partial Y}+\frac{\mu_{nf}}{\rho_{nf}\alpha_f}\left(\frac{\partial^2 V}{\partial X^2}+\frac{\partial^2 V}{\partial Y^2}\right)+\frac{(\rho\beta)_{nf}}{\rho_{nf}\beta_f}\mathrm{RaPr}\,\Theta \tag{3}$$

$$U\frac{\partial \Theta}{\partial X}+V\frac{\partial \Theta}{\partial Y}=\frac{\alpha_{nf}}{\alpha_f}\left(\frac{\partial^2 \Theta}{\partial X^2}+\frac{\partial^2 \Theta}{\partial Y^2}\right) \tag{4}$$

In the provided expressions, the subscripts "f" and "nf" refer to the fluid and nanofluid, respectively. ρ represents density, μ denotes dynamic viscosity, $C_p$ indicates specific heat, k represents thermal conductivity, and β stands for the coefficient of volume expansion. Since it is convenient to solve the governing equations in non-dimensional forms and hence, the following scales are used to get the non-dimensional governing equations:

$$X=\frac{x}{L},Y=\frac{y}{L},U=\frac{uL}{\alpha},V=\frac{vL}{\alpha},\mathrm{P}=\frac{pL^2}{\rho\alpha^2},\Theta=\frac{T-T_c}{T_h-T_c},\mathrm{Pr}=\frac{v}{\alpha},Ra=\frac{g\beta(T_h-T_c)L^3}{v\alpha}$$

where, x and y are the dimensional Cartesian coordinates, u and v are the dimensional velocity components in the x and y directions respectively, p is the dimensional pressure, T is the dimensional temperature and Th is the highest temperature of the bottom surface of the thick bottom wall, whereas X and Y are the dimensionless

coordinates, U and V are the dimensionless velocity components in the X and Y directions respectively, P is the dimensionless pressure, Θ is the dimensionless temperature, ρ is the density of fluid and α indicates thermal diffusivity of that fluid.
Conditions on all boundaries in dimensionless form are presented in Table 1. respectively.

**Table 1:** Boundary conditions in non-dimensional form

| Walls | Bottom and vertical walls | Top inclined walls | Heat source |
|---|---|---|---|
| Thermal Field | $d\theta/dx = 0$ | $\Theta = 0$ | $\Theta = 1$<br>$\Theta = 1\text{-}X$<br>$\Theta = \sin\pi x$ |
| Flow Field | | $U = V = 0$ | |
| Solid-fluid interface | | $(d\theta/dx)_{fluid}=R_c(d\theta/dy)_{solid}$ | |

The nanofluid effective properties are estimated using the effective medium theory as it provides a reasonable estimate of effective properties and this theory has been widely used for multiphase systems. The following expressions are used for the nanofluid effective properties:

$$\rho_{nf} = (1-\phi)\rho_f + \phi\rho_p \quad (5)$$

$$\left(\rho C_p\right)_{nf} = (1-\phi)\left(\rho C_p\right)_f + \phi\left(\rho C_p\right)_p \quad (6)$$

$$(\rho\beta)_{nf} = (1-\phi)(\rho\beta)_f + \phi(\rho\beta)_p \quad (7)$$

$$\mu_{nf} = \mu_f(123\phi^2 + 7.3\phi + 1) \quad (8)$$

$$k_{nf} = k_f(4.97\phi^2 + 2.72\phi + 1) \quad (9)$$

Table 2. lists the thermophysical characteristics of water and $Al_2O_3$ nanoparticles that were used to assess the $Al_2O_3$-water nanofluid's effective qualities for the numerical simulations

**Table 2:** Thermo physical properties of Water, $Al_2O_3$ nanoparticles and nanofluid at T = 20°C [13]

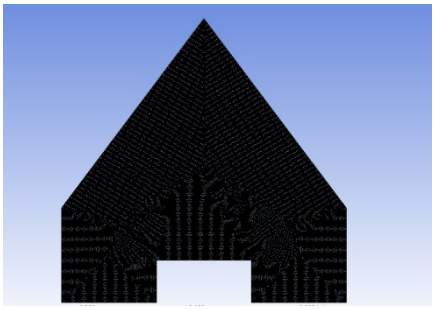
| **Variables** | **Water** | **$Al_2O_3$ nanoparticles** | **Nanofluid, $\phi$ = 4%** |
|---|---|---|---|
| $C_p$ [J/(kg.K)] | 4179 | 765 | 3705.04 |
| $\rho$ [kg/m$^3$] | 997.1 | 3970 | 1113.28 |
| $k$ [W/m.K] | 0.613 | 40 | 0.667 |
| $\beta$ [1/K] | $2.1\times10^{-4}$ | $8.5\times10^{-6}$ | $1.82\times10^{-4}$ |
| $\mu$ [kg/m] | $1.002\times10^{-3}$ | - | $1.48\times10^{-3}$ |
| $Pr$ [ - ] | 6.98 | - | 8.26 |

The mean dimensionless parameters governing the performance of this problem are average Nusselt number, Nu which is defined as follows:
Nusselt number can be calculated from

$$\mathrm{Nu} = -\int_0^1 \left(\frac{\partial\Theta}{\partial Y}\right)_{Y=\frac{t}{L}} dX$$

## "3. Simulation Procedure"

The Galerkin finite element method is used to solve the non-dimensional governing equations (eqs. 1-4) and the boundary conditions (Table 1). The computational domain is initially discretized using non-uniform triangular mesh pieces. The entire domain of prismatic enclosure is discretized into six nodded triangular mesh elements of different size. Different number of mesh elements are considered. The mesh elements taken for the simulation is 61278. The mesh diagram is given in Fig 2.



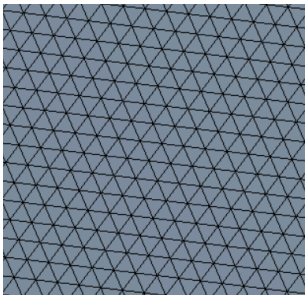


**Fig 2:** Triangular mesh generation in the prismatic enclosure. Extremely fine element is applied throughout the whole domain.

Subsequently, the grid independence test is carried out using a different number of mesh elements. 61278 elements with a node number of 31016 are chosen following the test for the current simulation because the average Nusselt number variation becomes insignificant with additional refinement. The computational code for every numerical simulation needs to be verified against the findings of some published literature. For this reason, we have contrasted our current research with Alam et al.'s earlier work. [9] A validation check was carried out by comparing the streamline, isotherm, and average result number plot observations. Plotting the average Nusselt number against Ra and comparing it to the findings of Alam et al. [9]—which are displayed in Fig. 4.4—provided additional validation. The outcomes of the current study agree with the findings of Alam et al.'s study [9].

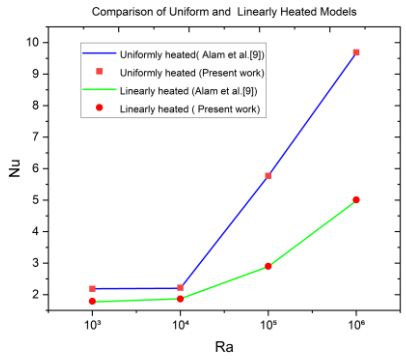
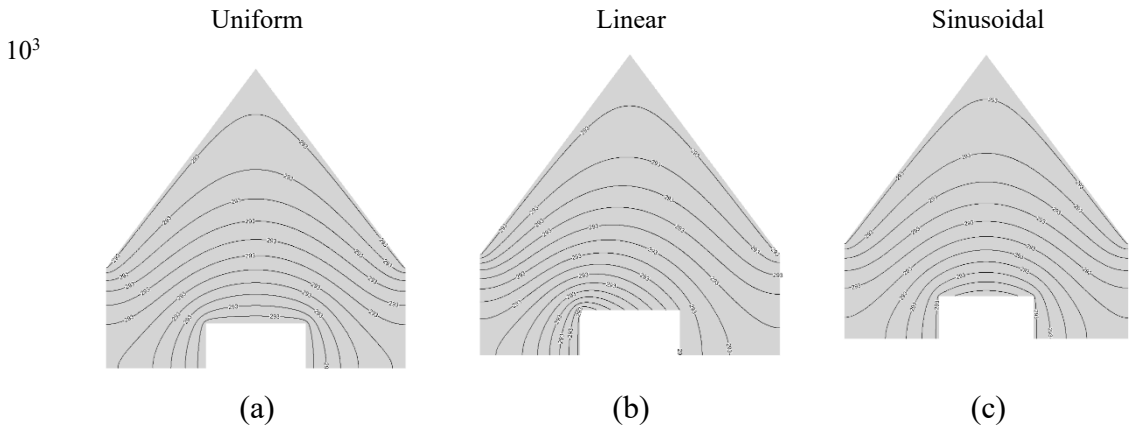



**Fig 3:** Validation of the model for prismatic enclosure with that of Alam *et al.* [9] for A = 1, uniformly and linearly heated bottom wall

## "4. Results and Discussions"

The contour plots of temperature, stream function, and entropy formation as a result of heat transfer are used in this part to illustrate some selected findings for the qualitative visualization of thermal and flow fields. In addition, the average Nusselt number distributions within the cavity are also provided to enable a comparative analysis of various thermal boundary conditions. Two distinct Rayleigh numbers, Ra = $10^3$ and $10^7$, are taken into consideration for three distinct heating circumstances applied at the prismatic cavity's bottom wall in order to present those qualitative results.



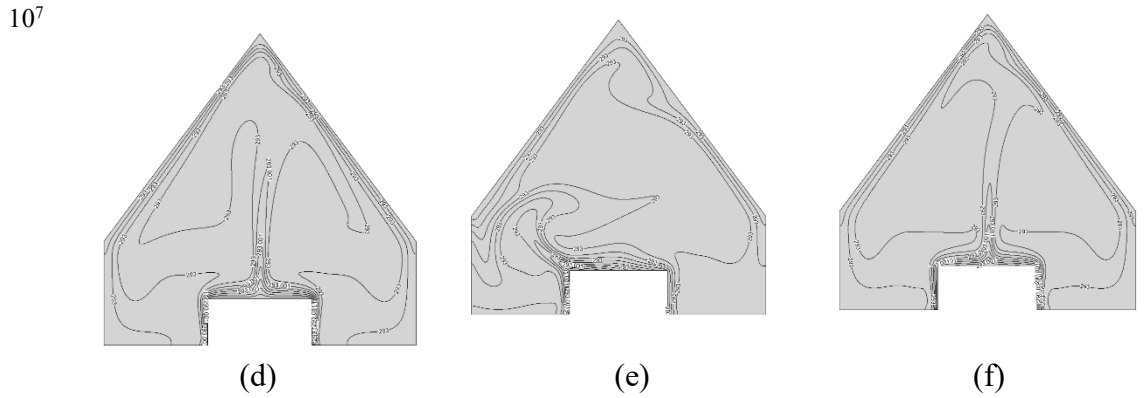



**Fig. 4**: Effects of Raleigh number on thermal field via isotherm plot for $Al_2O_3$ – water nanofluid for different heating conditions

Uniform heating shows weak vortices indicating conduction (Fig. 4a) and strong vortices with dominant convection (Fig. 4d). Linear heating features a single vortex representing simple circulation (Fig. 4b) and complex flow patterns with a strong primary and secondary vortex (Fig. 4e). Sinusoidal heating shows weak circulation with two vortices at low Ra (Fig. 4c), while high Ra results in vigorous convection with strong vortices (Fig. 4f)

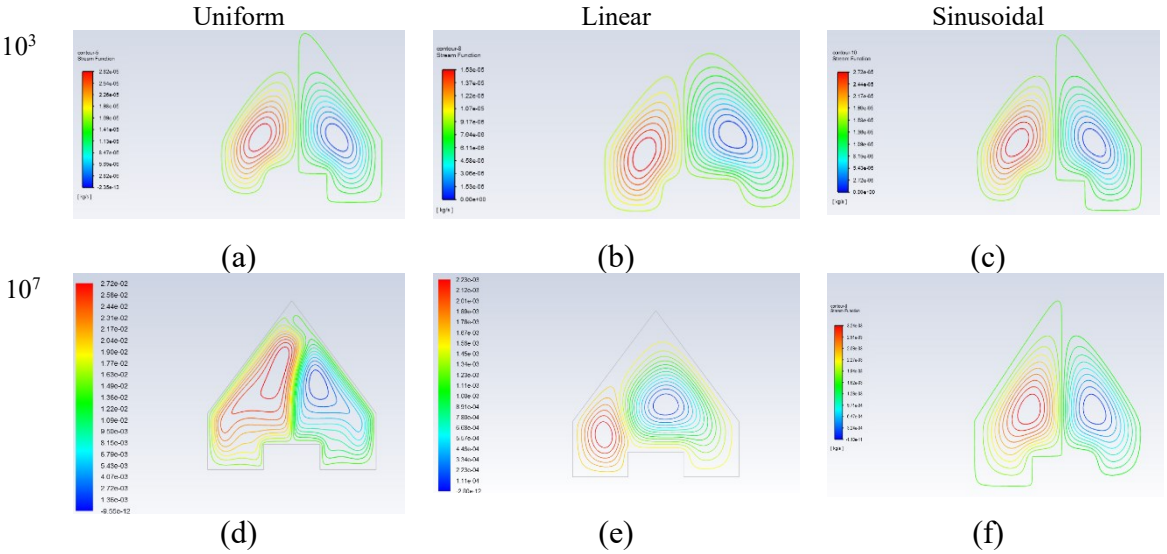
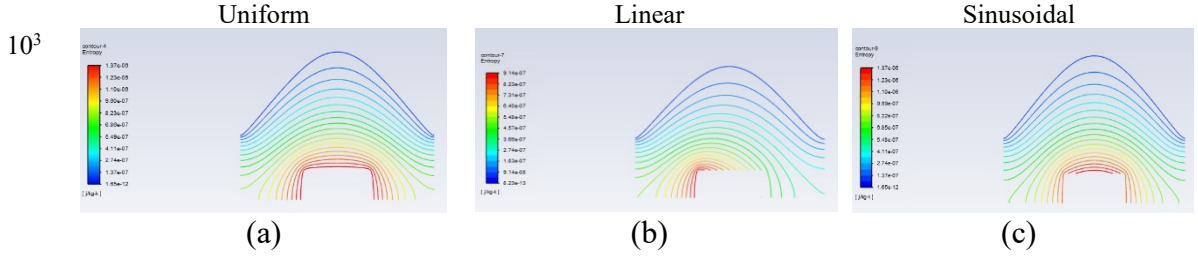
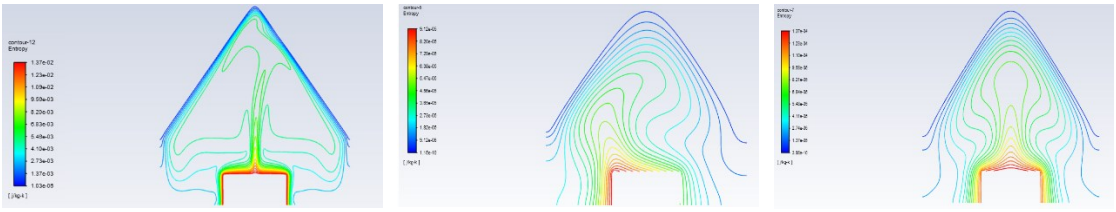



**Fig. 5**: Effects of Raleigh number on thermal field via streamline plot for $Al_2O_3$ – water nanofluid for different heating conditions

For uniform heating, Fig. 5(a) shows two weak vortices indicating conduction, while Fig. 5(d) displays strong and well-defined vortices, highlighting dominant convection. In linear heating, Fig. 5(b) features a single oval-shaped vortex, representing simple circulation with conduction, whereas Fig. 5(e) shows robust convection with a primary vortex and a secondary counter-clockwise vortex. Sinusoidal heating reveals two weak vortices at low Ra in Fig. 5(c), and vigorous circulation due to strong convection in Fig. 5(f).



$10^7$



(d) (e) (f)

**Fig. 6**: Effects of Raleigh number on thermal field via isentropic plot for $Al_2O_3$ – water nanofluid for different heating conditions

For uniform heating, Fig. 6(a) shows high entropy generation ($S_\Theta$) at the corners due to conduction, while Fig. 6(d) indicates minimal entropy generation, suggesting efficient heat transfer at high Ra. In linear heating, Fig. 6(b) reveals high $S_\Theta$ near the left wall, indicating strong local heat transfer, whereas Fig. 6(e) shows minimal entropy generation in the center, reflecting efficient convection. Sinusoidal heating displays high $S_\Theta$ at the corners in Fig. 6(c), indicating large thermal gradients, while Fig. 6(f) shows significant entropy generation near the bottom wall due to strong convection.

The Nusselt number represents the ratio of heat transmitted by fluid by conduction to that transferred through fluid motion. The top surface of the thick bottom wall is used to measure differences in the average Nusselt number in this instance. The distribution of the average Nusselt number as a function of Rayleigh number for the enclosure containing $Al_2O_3$-water nanofluid is shown in Fig 7. Fig 7 shows that, under all heating conditions, the Nusselt number is independent of the Rayleigh number up to Ra = $10^4$. An increase in the Rayleigh number further indicates a slow growth in the Nusselt number. A higher Rayleigh number improves the enclosure's overall flow. Thus, as Fig 7 clearly illustrate, the Nusselt number should be increased in the Rayleigh number zone ($10^4 \leq Ra \leq 10^7$). It is also evident that, as would be expected, a bottom wall case that is heated uniformly exhibits the maximum heat transfer rate. For the heat source, we chose highly conductive material. In the low Rayleigh number zone, it is evident that conduction will take precedence over convection when this conductive substance is added.

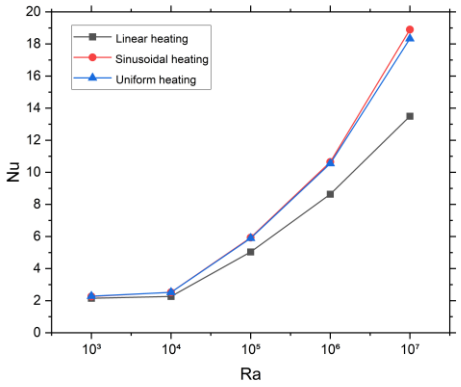



**Fig 7:** Variation of Nusselt number with Ra for $Al_2O_3$– water nanofluid

## "5. Conclusions"

This study explores natural convection of a water-Al2O3 nanofluid inside a prismatic cavity with a thick bottom wall, subject to three different heating conditions: isothermal, linear, and sinusoidal. The results show that higher Rayleigh numbers enhance nanofluid mixing, especially with sinusoidal heating, improving heat transfer.

## "6. References"


[1] Y. A. Cengel, Heat Transfer; A Practical Approach, 2nd ed.

[2] Basak, Tanmay, S. Roy and I. Pop, "Heat flow analysis for natural convection within trapezoidal enclosures based on heatline concept," *International Journal of Heat and Mass Transfer,* vol. 52, no. 11-12, pp. 2471-2483, 2009.

[3] Oliveski, R. D. C, M. H. Macagnan and J. B. Copett, "Entropy generation and natural convection in rectangular cavities," *Applied Thermal Engineering,* vol. 29, no. 8-9, pp. 1417-1425, 2009.

[4] Jou, R. Yuan and S. C. Tzeng, "Numerical research of nature convective heat transfer enhancement filled with nanofluids in rectangular enclosures," *International Communications in Heat and Mass Transfer ,* vol. 33, no. 6, pp. 727-736, 2006.

[5] Raisi, "Heat transfer in an enclosure filled with a nanofluid and containing a heat-generating conductive body," *Applied Thermal Engineering,* vol. 110, pp. 469-480, 2017.

[6] Sharifpur, Mohsen, A. B. Solomon, T. L. Ottermann and J. P. Meyer, "Optimum concentration of nanofluids for heat transfer enhancement under cavity flow natural convection with TiO2–Water," *International Communications in Heat and Mass Transfer,* vol. 98, pp. 297-303, 2018.

[7] Shuja, S. Z., B. S. Yilbas and M. O. Iqbal, "Mixed convection in a square cavity due to heat generating rectangular body: Effect of cavity exit port locations.," *International Journal of Numerical Methods for Heat & Fluid Flow,* vol. 10, no. 8, pp. 824-841, 2000.

[8] Jafari, Mohammad, M. Farhad, S. Akbarzade and M. Ebrahimi, "Lattice Boltzmann simulation of natural convection heat transfer of SWCNT-nanofluid in an open enclosure," *Ain Shams Engineering Journal,* vol. 6, no. 3, pp. 913-927, 2015.

[9] M. S. Alam, M. M. Rahman, S. Parvin and K. Vajravelu, "Finite Element Simulation for Heatline Visualization of Natural Convective Flow and Heat Transfer inside a Prismatic Enclosure," *International journal of heat and technology,* vol. 34, no. 3, pp. 391-400, 2016.

[10] Aich, Walid, I. Hajri and A. Omri, "Numerical analysis of natural convection in a prismatic enclosure," *Thermal science,* vol. 15, no. 2, pp. 437-446, 2011.

[11] Quintino, Alessandro, M. Cianfrini, P. Ocłoń, E. Ricci and M. Corcione, "Buoyancy-induced convection of water-based nanofluids from an enclosed heated cylinder," *International Journal of Numerical Methods for Heat & Fluid Flow,* vol. 28, no. 11, pp. 2734-2755, 2018.

[12] J. S. Yaseen, "Numerical Analysis of Steady Natural Convection in a Prismatic Enclosure with Strip Heater on Bottom Wall Using Flexpde," *Diyala Journal of Engineering and Sciences,* vol. 7, no. 2, pp. 61-80, 2014.

[13] Y. Xuan and Q. Li, "Heat transfer enhancement of nanofluids," *International Journal of Heat and Fluid Flow,* vol. 21, no. 1, pp. 58-64, 2000.